AJNR Am J Neuroradiol 26:229–235, February 2005

Diffusion Abnormality of Deep Gray Matter in External Capsular Hemorrhage

Won-Jin Moon, Dong Gyu Na, Sam Soo Kim, Jae Wook Ryoo, and Eun Chul Chung

BACKGROUND AND PURPOSE: **To our knowledge, diffusion abnormality of the unaffected deep gray matter during striatocapsular hemorrhage has not been previously described in the literature. We report the presence of the diffusion abnormality separated from hematoma in patients with external capsular (lateral striatocapsular) hemorrhage and suggest the plausible mechanisms of diffusion signal intensity change.**

METHODS: **We retrospectively reviewed MR images in 28 consecutive patients with spontaneous striatocapsular hemorrhage and evaluated signal intensity changes at sites separated from the hemorrhage and the lesions on diffusion-weighted (DW) images. Apparent diffusion coefficients (ADCs) of the lesions were measured, and volume changes in the deep gray matter were assessed at follow-up.**

RESULTS: **On DW images, hyperintensity of deep gray matter was found in nine patients (25%). In all patients with DW imaging abnormality, the hemorrhage was located in the external capsule, and the interval from hemorrhagic ictus to MR imaging study was 8–54 days. Hyperintensity of the deep gray matter was seen in the caudate ($n = 8$), putamen ($n = 7$), thalamus ($n = 5$), and substantia nigra ($n = 2$). Mean relative ADC ratios of the diffusion abnormality were 0.76 ± 0.10 in the caudate, 0.79 ± 0.07 in the putamen, and 0.85 ± 0.11 in the thalamus. DW imaging abnormality disappeared with mild atrophy in two patients who underwent follow-up imaging.**

CONCLUSION: **External capsular hemorrhage may be uncommonly accompanied by diffusion abnormality in the striatum or thalamus at follow-up, and the lesion should not be misdiagnosed as new-onset infarction. Secondary neuronal degeneration may play an important role in the development of diffusion abnormality.**

Spontaneous intracerebral hemorrhage (ICH) accounts for 10% of all strokes and is associated with mortality and morbidity rates higher than those of cerebral infarction (1). Spontaneous ICH can be classified into two types: deep hemorrhage, which is classically associated with hypertension, and lobar hemorrhage, which may result from cerebral amyloid angiopathy (1). The hypertensive hemorrhage of the striatocapsule is most frequently encountered in daily practice (2).

Although nonenhanced CT has been the diagnostic technique of choice for ICH, the use of MR imaging has recently expanded. The different stages of ICH can be easily determined by analyzing the appearance its various patterns on MR images. With the advent of diffusion-weighted (DW) imaging, valuable additional information about ICH, especially features to differentiate hemorrhage from infarction in hyperacute stroke, can be obtained (3–6).

In addition to the study of the hematoma itself, the accompanying abnormality of ICH on DW imaging has been investigated (7–11). Wallerian degeneration of the corticospinal tract after ICH can be depicted earlier on DW imaging than on conventional MR imaging (9, 10). Several reports suggest that perihematoma ischemia or perihematoma edema can be identified on DW imaging (7, 8, 11).

We observed diffusion abnormalities in the caudate nucleus and putamen of patients with external capsular (lateral striatocapsular) hemorrhage; these abnormalities were separated from the bleeding site and the rim of perihematoma edema. To our knowledge, only one report has described this diffusion abnormality separated from the hematoma (12). We performed this retrospective study to determine the presence of the diffusion abnormality separated from

Received December 31, 2003; accepted after revision June 3, 2004.

From the Department of Radiology, Kangbuk Samsung Hospital (W.-J.M., E.C.C.) and Samsung Medical Center (S.S.K., J.W.R.), Sungkyunkwan University School of Medicine, Seoul National University Hospital (D.G.N.), Seoul, Korea.

Address reprint requests to Dong Gyu Na, MD, Department of Radiology, Seoul National University Hospital, 28 Yongon-Dong, Chongno-gu, Seoul 110-744, Korea, email: dgna@radiol.snu.ac.kr.

hematoma in patients with striatocapsular hemorrhage and to suggest the plausible mechanisms of signal intensity change on DW imaging.

Methods

Patients

We collected clinical and imaging data in 36 consecutive patients who had spontaneous hemorrhage in the basal ganglia (striatocapsule) and who were referred for MR imaging from our departments of neurology and neurosurgery. The patients' records were retrieved from the electronic database of our medical center between 1999 and 2001. Patients with arteriovenous malformation, aneurysm, or tumor as the underlying cause of hemorrhage were excluded. Of the 36 patients with spontaneous striatocapsular hemorrhage, 28 patients (14 women and 14 men aged 17–74 years; median age, 57 years) were included, whereas eight patients were excluded because of a lack of diffusion imaging. The presence of intracerebral hematoma was determined by means of CT in 26 patients and by means of gradient-echo MR imaging in two patients. Surgery for stereotaxic aspiration was performed in six patients, and open surgery was performed in four patients.

MR imaging studies were performed at various intervals after hemorrhagic ictus. Five ICH stages were defined according to the interval between hemorrhagic ictus and initial MR imaging examination, as follows: Acute was 0–3 days ($n = 4$), early subacute was 4–7 days ($n = 5$), late subacute was 8–30 days ($n = 11$), early chronic was 31–60 days ($n = 2$), and late chronic was 61 days or longer ($n = 6$). Follow-up MR imaging was performed in seven patients, and follow-up CT was performed in two, with intervals varying from 2 to 25 months (median, 8 months). The patients' medical records were reviewed to evaluate their neurologic status at the time of MR imaging.

MR Imaging

A 1.5-T unit (Signa; GE Medical Systems, Milwaukee, WI) was used for MR imaging. The conventional MR imaging protocol included the following sequences: 1) axial T1-weighted spin-echo (TR/TE, 467/9), 2) axial T2-weighted fast spin-echo (TR/effective TE, 3417/102), and 3) axial fluid-attenuated inversion recovery (FLAIR; TR/TE/TI, 10,000/140/2200). Parameters for conventional MR imaging were a matrix of 256 × 192, a 23-cm field of view, and a 5-mm section thickness and 2-mm intersection gap. Single-shot spin-echo echo-planar DW imaging sequences were obtained by applying diffusion gradients in three orthogonal directions for each section, with two diffusion weightings ($b = 0$ s/mm^2 and $b = 900$ or 1000 s/mm^2). Isotropic DW imaging was generated online by averaging three orthogonal-axis images. During DW imaging 20 sections were acquired with these parameters: TR/TE of 6500/96.8, matrix of 128 × 128, field of view of 28 cm, and section thickness of 5 mm, and intersection gap of 2 mm. In addition, conventional T2*-weighted gradient-echo imaging (TR/TE, 450/20) was performed in 22 of the 28 patients.

Imaging Analysis

Two neuroradiologists (W.-J.M., D.G.N.) retrospectively reviewed the presence and location of the diffusion abnormality in the deep gray matter in each patient. By consensus, we determined the presence of DW imaging abnormality when high signal intensity was present in the deep gray matter on DW imaging. The DW imaging abnormality did not overlap with the hematoma or perihematoma edema and did not surround the hematoma. Signal intensity changes on conventional MR images were also evaluated and compared with those seen on the DW images. The location of the ICH was categorized into six types based on vascular territory, as Chung et al suggested (2): 1) anterior (Heubner artery), 2) middle (medial lenticulostriate artery), 3) posteromedial (posteromedial branches of the lateral lenticulostriate artery), 4) posterolateral (posterolateral branches of the lateral lenticulostriate artery), 5) lateral (most lateral branches of the lateral lenticulostriate artery), and 6) massive. Figure 1 shows a schematic diagram based on the classification of striatocapsular hemorrhage (2). The diagram shows that lateral type of striatocapsular hemorrhage primarily involved the external capsular area between lateral putamen and insular cortex. Therefore, we designated the lateral type of striatocapsular hemorrhage as external capsular hemorrhage.

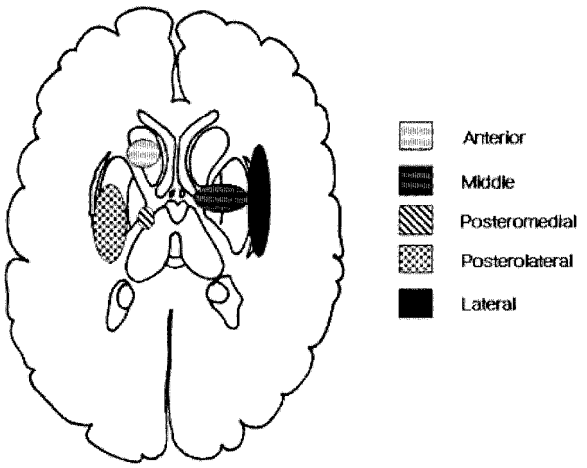

FIG 1. Schematic classification of striatocapsular hemorrhage.

Quantitative analysis of apparent diffusion coefficients (ADCs) and signal intensity on DW imaging was performed in hyperintense lesions in the deep gray nuclei that were separated from the hematoma. A region of interest (ROI) was placed in the caudate, putamen, and thalamus bilaterally by carefully excluding perihematoma edema and the hematoma itself. The ROI ranged from 16 to 302 mm^2, and in each case, a neuroradiologist (W.-J.M.) measured the ROI. ADC values were calculated according to the following equation: $ADC = (\ln S_2 - \ln S_1)/b$, where S_1 is ROI signal intensity with diffusion gradients, S_2 is the ROI signal intensity without diffusion gradients, and b is the difference in b value between images with ($b = 900$ or 1000 s/mm^2) and images without ($b = 0$ s/mm^2) diffusion-sensitizing gradients. The relative ADC ratio (the ratio of the ADC value for a lesion to that of normal contralateral gray matter) was also calculated in each case. All data for ADC values and relative ADCs for each stage are presented as the mean ± 1 SD.

Volume measurements of the hematoma were obtained with initial CT performed within a day of symptom onset. Hematoma volumes were measured by using a simplified formula for the volume of ellipsoid: $\frac{ABC}{2}$, where A is the largest diameter of the hemorrhage on the section on which the largest area of hemorrhage was identified, B is the largest diameter oriented 90° to A on the same section, and C is the approximate number of sections on which the ICH was seen. Volume analysis was not performed in two patients whose initial CT images were not available; the hemorrhage, however, was confirmed on gradient-echo MR images.

To determine whether the deep gray matter involved on DW imaging had atrophied, the volume of the caudate and the thalamus was obtained. The putamen was excluded from the volume analysis because its size could not be measured without inadvertent inclusion of the adjacent hematoma and edema. To evaluate the chronologic changes in size, a difference of up to ±5% was allowed when the size of deep gray matter was compared on initial and follow-up images. This consideration

TABLE 1: Clinicoradiologic data in patients with diffusion abnormality remote from ICH

Patient/Sex/Age (y)	Time after ICH (days)	Location of ICH	Treatment	Hyperintensity	
				DWI	FLAIR Imaging
1/M/33	40	R EC	Surgical	C, P, T, SN	C, P, T, SN
2/M/52	27	L EC	Surgical	C, P, T	C, P, T
3/F/55	28	R EC	Surgical	C, T, SN	C, T
4/M/51	24	R EC	Conservative	P	P
5/F/51	8	R EC	Surgical	C, P	C, P
6/F/78	54	L EC	Conservative	C, T	C, T
7/M/70	17	L EC/T	Surgical	C, P	C, P
8/M/66	30	L EC	Surgical	C, P, T	C, P, T
9/M/74	16	R EC	Conservative	C, P, T	C, P, T

Note.—C is the caudate nucleus head; EC, external capsule; P, putamen; SN, substantia nigra; and T, thalamus.

accounted for calculation errors and slight differences in the position of brain sections at different time points.

Statistical Analysis

SPSS (version 10.1; SPSS Inc, Chicago, IL) was used for statistical analysis. The Mann-Whitney or Kruskal-Wallis test was used to determine differences in ADC values, ADC ratios, and initial ICH volumes between the abnormal and normal DW imaging groups. Clinical and radiologic findings were analyzed with the Fisher exact test. The level of significance was defined at $P < .05$.

Results

Clinicoradiologic Characteristics of the Abnormal DW Imaging Group

Table 1 summarizes the clinicoradiologic data of the patients whose images showed diffusion abnormality in the deep gray matter. Nine of the 28 patients with striatocapsular hemorrhage had DW imaging abnormalities in the deep gray matter, all in association with the lateral type (external capsular hematoma). At the time of the MR imaging study, no patient presented with acute neurologic deficits suggestive of any acute infarction.

In the abnormal DW imaging group ($n = 9$), six patients (67%) underwent surgery, whereas only three patients (16%) in the normal DW imaging group ($n = 19$) had surgery. DW imaging abnormalities were found only in patients with late subacute hematoma ($n = 7$) or early chronic hematoma ($n = 2$) (Table 2). Unlike the lateral type of striatocapsular hematoma, the posterolateral or anterior type of striatocapsular hematoma, which primarily involved lateral basal ganglia, did not result in diffusion abnormality (Table 3). The age and location of the hemorrhages significantly differed between the abnormal and normal DW imaging groups ($P < .05$). In the abnormal DW imaging group, the caudate head ($n = 8$) was the area most commonly affected, followed by the putamen ($n = 7$), the thalamus ($n = 6$), and the substantia nigra ($n = 2$) (Fig 2). FLAIR imaging revealed subtle high signal intensity in the caudate nucleus ($n = 8$), putamen ($n = 7$), and thalamus ($n = 6$).

TABLE 2: Relationship between DWI abnormality and interval after hemorrhage onset

Interval (days)	DWI Finding		
	Abnormal	Normal	Total
0–3	0	4	4
4–7	0	5	5
8–30	7	4	11
31–60	2	0	2
61 or more	0	6	6
Total	9	19	28

ADCs and Chronologic Changes in DW Imaging Hyperintensity

When DW imaging showed abnormally high signal intensity in any region of the caudate head, putamen, or thalamus, the ADC value and the ADC ratio relative to the contralateral gray matter decreased significantly ($P < .05$) (Table 4). Two of nine patients with DW imaging abnormalities underwent follow-up DW imaging (8 and 10 months after symptom onset) (Table 4). Follow-up images in both showed complete reversal of the DW imaging hyperintensity (Fig 3). ADC values and ADC ratios normalized on follow-up.

Comparison of Initial Hematoma Volume and Atrophy of Ipsilateral Gray Matter on Follow-Up

The abnormal DW imaging group ($n = 9$) had a volume of initial ICH significantly larger than that of the normal DW imaging group ($n = 17$) (33.24 ± 11.83 vs. 13.24 ± 11.20 10^3 mm^3; $P = .001$). To evaluate whether the hematoma volume independently affected the presence of diffusion abnormality, we compared the volumes of hematoma with different locations and then compared the hematoma volumes between patients with lateral striatocapsular hemorrhage with and without diffusion abnormality. In all patients with and those without diffusion abnormality, the lateral type of striatocapsular hemorrhage result in a significantly larger volume of hematoma ($P = .001$). In all patients with the lateral type of striatocapsular hemorrhage, hematoma volume was significantly larger in patients with diffusion ab-

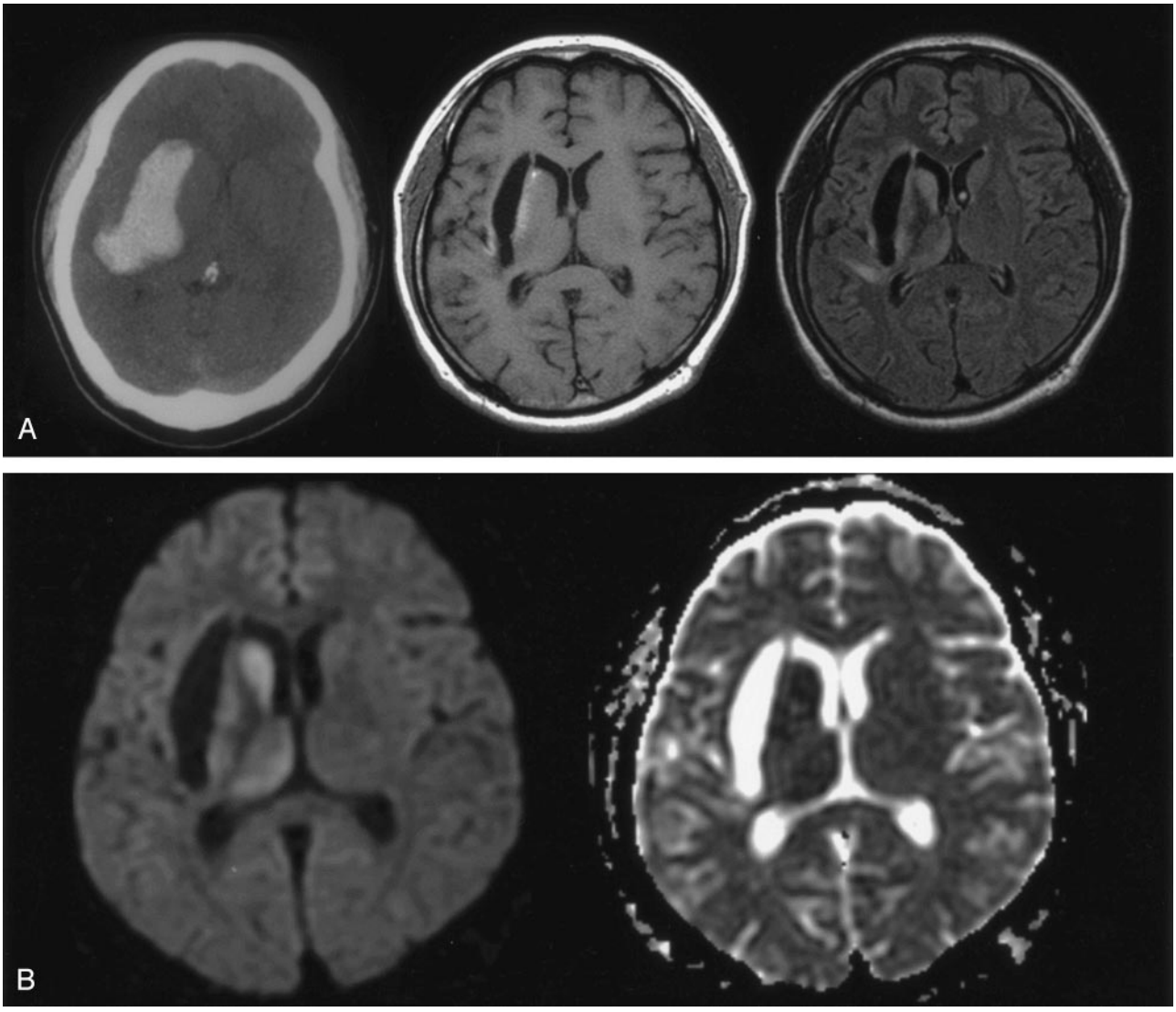

FIG 2. Patient 1. A 33-year-old man with early chronic intracerebral hematoma on MR images obtained 40 days after symptom onset.
A, CT scan (*left*) 12 days after symptom onset shows a hyperattenuating hematoma primarily in the right external capsule between the lateral putamen and the insular cortex. T1-weighted image (*middle*) shows a hypointense cavitary lesion in the right external capsule. FLAIR image (*right*) reveals subtle hyperintensity of the deep gray matter in the caudate head, putamen, thalamus, and part of the insular cortex.
B, Diffusion-weighted image (*left*) shows obvious hyperintensity in the caudate head, putamen, and thalamus, which are separate from the hematoma itself. No other diffusion abnormality is seen. ADC map (*right*) shows decreased ADC in the caudate, putamen, and thalamus; ADC ratios relative to contralateral gray matter were 0.75, 0.79, and 0.80, respectively. This suggests that the diffusion abnormality is impaired intracellular diffusion rather than a T2 shine-through effect.

TABLE 3: Relationship between DWI abnormality and location of the hemorrhage

	DWI Finding		
Location	Abnormal	Normal	Total
Lateral	9	7	16
Posterolateral	0	10	10
Anterior	0	2	2
Total	9	19	28

TABLE 4: Relationship between DWI abnormality and ADC change

Location and DWI Finding	ADC (10^{-6} mm/s)	ADC Ratio	*P* Value
Caudate			.000
Abnormal (n = 8)	582 ± 135	0.76 ± 0.10	
Normal (n = 19)	857 ± 152	1.03 ± 0.18	
Putamen			.000
Abnormal (n = 8)	612 ± 68	0.79 ± 0.07	
Normal (n = 19)	821 ± 151	1.04 ± 0.13	
Thalamus			.028
Abnormal (n = 5)	650 ± 68	0.85 ± 0.11	
Normal (n = 22)	820 ± 75	1.00 ± 0.07	

normality than in patients with no diffusion abnormality (P = .040).

Follow-up MR images were obtained in two patients in the abnormal DW imaging group and in two patients in the normal DW imaging group. In abnormal DW imaging group, a significant reduction in volume was noted in the caudate (19–34%) and thal-

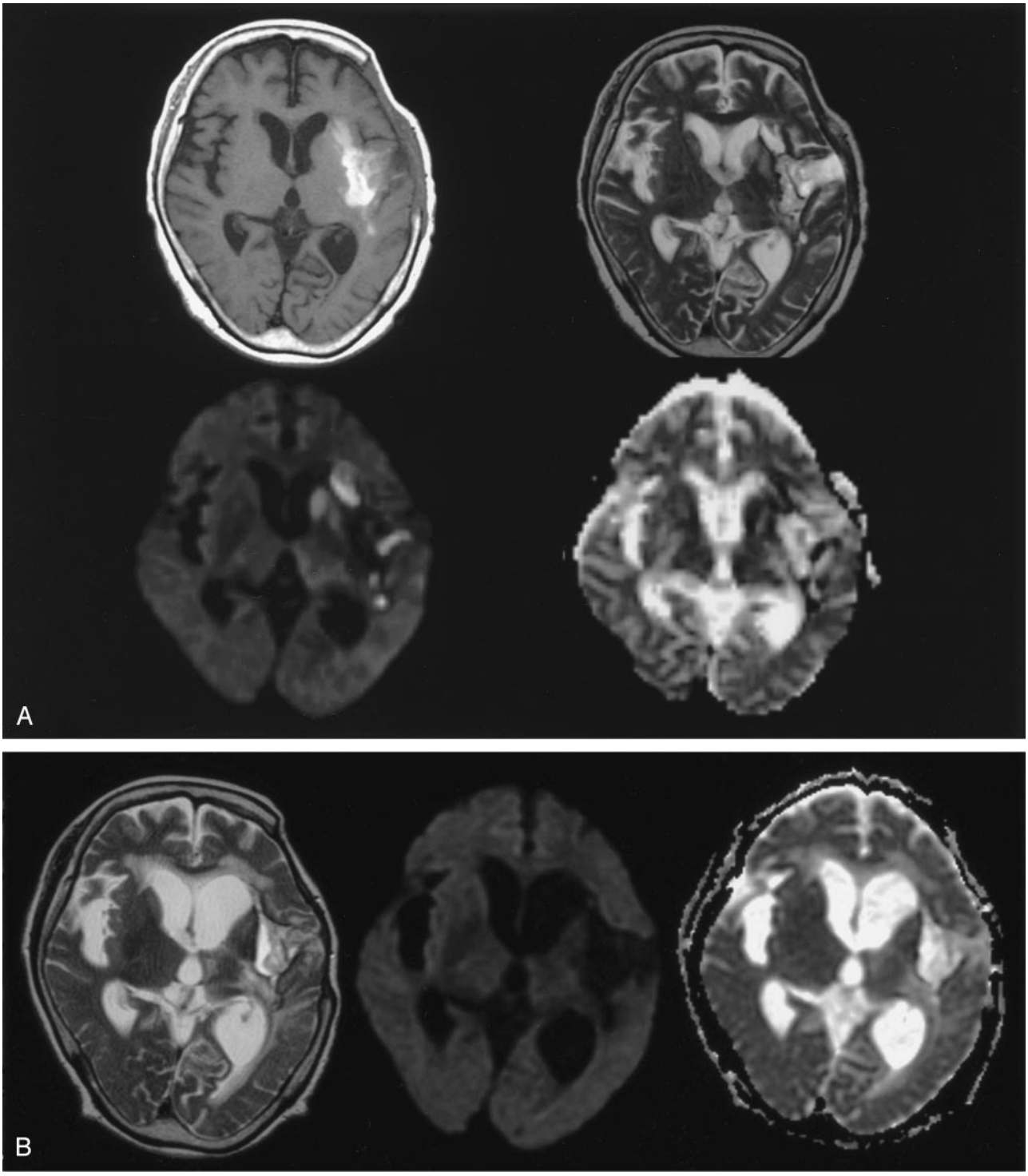

FIG 3. Patient 8. A 66-year-old man with late subacute intracerebral hematoma on MR images obtained 30 days after symptom onset.

A, T1-weighted image (*top left*) shows hyperintensity of the hematoma mainly in the left external capsule area. Hematoma also extends into a part of the posterior angle of the putamen and insular cortex. T2-weighted image (*top right*) shows the hematoma as a hyperintense area circumscribed by a hypointense rim; this suggests subacute hematoma. Subtle hyperintensity is noted in the ipsilateral caudate head and putamen. DW image (*bottom left*) shows obvious hyperintensity in the caudate and putamen and mild hyperintensity in the thalamus. ADC map (*bottom right*) shows decreased ADC in the caudate, part of the putamen and medial-posterior thalamus; ADC ratios relative to the contralateral gray matter were 0.59, 0.61, and 0.87, respectively.

B, T2-weighted image (*left*) obtained 12 months later shows atrophy of the caudate and putamen, while the hematoma resolves to a slitlike cavity. Follow-up diffusion image (*middle*) reveals no definable signal intensity change in the caudate, putamen, or thalamus ipsilateral to the hematoma. Follow-up ADC map (*right*) shows normalization of ADC values in the corresponding deep gray matter.

amus (16–18%). On the contrary, the normal DW imaging group showed minimal volume reduction (2–4% in the caudate and 5–7% in the thalamus).

Discussion

In the present study, hyperintensity of the deep gray matter was found on DW imaging in nine (32%) of 28 patients with striatocapsular hemorrhage. These DW imaging abnormalities were found exclusively in the external capsular hemorrhage in the subacute stages. On follow-up, the deep gray matter with diffusion abnormality showed significant atrophic change.

Interestingly, all patients with DW imaging abnormalities had ICH in the external capsule between the insular cortex and the lateral margin of the putamen. Although the external capsule is not part of the basal ganglia, hemorrhage of the external capsule has been long regarded as the lateral type of striatocapsular hemorrhage (2). The hemorrhage mainly involving external capsule results in an ellipsoid mass of maximal anteroposterior diameter along the white matter pathways. This type does not directly affect the putamen but often compresses the middle portion of the putamen (2). Despite their relatively large hematoma, patients with the lateral type presented with a benign clinical course and were therefore treated medically (2). Why these diffusion abnormalities were seen exclusively in patients with the external capsular hemorrhage is unclear.

Diffusion abnormality separated from ICH resulted in the atrophy of the affected area on follow-up imaging study. The resultant atrophy of the previous diffusion abnormality suggests structural change in the affected area. These characteristics of DW imaging abnormality in the deep gray matter in cases of striatocapsular hemorrhage suggest possible underlying mechanisms for the diffusion abnormality after hemorrhage, such as secondary transneuronal degeneration (13, 14), ischemic change by direct compression (15–17), and inflammatory reaction (18, 19).

Neuronal damage caused by a focal brain lesion influences function and morphology in regions intact after the primary injury (13, 14, 20–23). The classic forms of neuronal degeneration are wallerian and transneuronal. Wallerian degeneration is afferent axonal degeneration occurring after injury to the axon or cell body; this type does not extend to other neurons. On the contrary, transneuronal degeneration involves both afferent and efferent neurons through synaptic connections (13, 14). Cerebral infarction in the territory of the middle cerebral artery can cause transneuronal degeneration in the substantia nigra and the thalamus, which have transsynaptic connections with the caudoputamen and the cerebral cortex, respectively (24, 25–27). In this study, diffusion abnormalities after external capsular hemorrhage were observed in the substantia nigra and thalamus, as well as in the striatum. We can speculate that a mechanism analogous to that of transneuronal degeneration may be behind the diffusion abnormality remote from ICH.

Major afferents to the striatum are derived from the cerebral cortex, thalamus, and substantia nigra (28). Major efferents from the striatum terminate at the globus pallidus and substantia nigra. Although the structure of external capsule is not entirely known, it is thought to contain corticostriate fibers connecting the cerebral cortex and the striatum (28). Regarding the striatum, antegrade neuronal degeneration of the corticostriate fibers has not been reported, while retrograde degeneration is reported in the external capsule after the necrosis of the striatum (27). As both antegrade and retrograde transneuronal degeneration are possible after any neuronal injury, external capsular lesion may induce antegrade neuronal degeneration involving the striatum.

Unlike the caudate and the putamen, the thalamus and the substantia nigra do not contain a direct connection with the external capsule. The thalamus contains thalamostriate fibers to the striatum; these may be the target of retrograde neuronal degeneration due to striatal injury (14). The substantia nigra has both afferent and efferent connections to the striatum. Therefore, both antegrade and retrograde neuronal degeneration of the substantia nigra may be possible after striatal injury.

Although decreased ADC in secondary neuronal degeneration is unclear, axonal swelling (28) and cellular swelling of astrocytic endplate and neurons (24, 29) could be the major causes of impaired intracellular diffusion resulting in decreased ADC.

The exact timing of diffusion abnormality in transneuronal degeneration is still unknown, while diffusion abnormality of wallerian degeneration is known to develop even within 2 days after injury (30). In an animal study, transneuronal degeneration resulted in decreased ADC 3 days after injury (24). We observed the diffusion abnormalities mostly in the subacute stage.

Another possibility for diffusion abnormality may be cytotoxic edema caused by ischemic change due to vascular compromise after ICH. The underlying cause for vascular compromise may be direct compression of the hematoma (15–17). The caudate nucleus and the putamen are highly cellular and well-vascularized zones permeated by delicate bundles of finely myelinated or nonmyelinated small-diameter fibers (28). The external capsule is a relatively narrow zone exposed to the hemorrhage induced by hypertension, as compared the with parietal or frontal subcortical white matter. Therefore, external capsular hemorrhage may exert enough pressure on the neighboring caudate and putamen to compromise their fine vasculature. Our finding of substantially more hematoma in the abnormal DW imaging group than in the normal DW imaging group supports this theory. However, the major drawback of this theory is the timing of the diffusion abnormality. Maximum mass effect from the hematoma occurs within the first week, and therefore, it is difficult to explain the diffusion abnormality noted in the subacute and chronic stages. Furthermore, the theory of direct ischemic injury by compression cannot explain the diffusion abnormality in the substantia nigra and the thalamus, which are remote from the ICH in some patients.

Another possible reason for the diffusion abnormality may be inflammation induced by intracerebral hematoma (18, 19). ICH causes adjacent parenchymal inflammation within hours of its occurrence; this is initiated by the adherence by leukocytes to damaged brain endothelia and their subsequent entry in to the brain (18). Although levels of most inflammatory molecules are increased immediately after ICH, one report (19) describes an increase in some inflammatory molecules at a week after ICH. This might explain the delayed diffusion abnormality after ICH. Nevertheless, the inflammation cannot explain the diffusion abnormality in the thalamus and midbrain, which are separated from the initial hematoma.

In cases of external capsular hemorrhage, diffusion abnormality in the ipsilateral deep gray matter may mimic an acute ischemic lesion due to another cause. No clinical evidence suggests any new acute ischemic insult, and the distribution of sites of diffusion abnormality indicates that decreased ADC in the deep gray matter is not caused by any incidental acute infarction not associated with ICH. Therefore, the DW imaging abnormality in this study was not due to acute infarction, but rather, a delayed injury accompanying the hemorrhage.

Our study had some limitations. First, histopathologic correlation with diffusion abnormality was lacking. Animal experiments may be helpful in widening our knowledge on diffusion abnormality and its mechanism after ICH. Second, this study was not prospective but retrospective, and we obtained follow-up MR images in only a limited number of patients. Prospective study with serial observation may be required to determine the clinical relevance of diffusion abnormality after external capsular ICH.

Conclusion

Diffusion abnormalities in the ipsilateral gray matter after external capsular ICH are uncommon and leave residual localized atrophy. Secondary neuronal degeneration may be suggested as a plausible mechanism. Diffusion abnormality of the caudoputamen or thalamus should not be misdiagnosed as new-onset infarction on follow-up MR imaging in patients with external capsular hemorrhage.

References

1. Labovitz DL, Sacco RL. **Intracerebral hemorrhage: update.** *Curr Opin Neurol* 2001;14:103–108
2. Chung CS, Caplan LR, Yamamoto Y, et al. **Striatocapsular hemorrhage.** *Brain* 2000;123:1850–1862
3. Schellinger PD, Jansen O, Fiebach JB, Hacke W, Sartor K. **A standardized MRI stroke protocol: comparison with CT in hyperacute intracerebral hemorrhage.** *Stroke* 1999;30:765–768
4. Atlas SW, DuBois P, Singer MB, Lu D. **Diffusion measurements in intracranial hematomas: implications for MR imaging of acute stroke.** *AJNR Am J Neuroradiol* 2000;21:1190–1194
5. Kang BK, Na DG, Ryoo JW, Byun HS, Roh HG, Pyeun YS. **Diffusion-weighted MR imaging of intracerebral hemorrhage.** *Korean J Radiol* 2001;2:183–191
6. Wiesmann M, Mayer TE, Yousry I, Hamann GF, Bruckmann H. **Detection of hyperacute parenchymal hemorrhage of the brain using echo-planar T2*-weighted and diffusion-weighted MRI.** *Eur Radiol* 2001;11:849–853
7. Carhuapoma JR, Wang PY, Beauchamp NJ, Keyl PM, Hanley DF, Barker PB. **Diffusion-weighted MRI and proton MR spectroscopic imaging in the study of secondary neuronal injury after intracerebral hemorrhage.** *Stroke* 2000;31:726–732
8. Carhuapoma JR, Barker PB, Hanley DF, Wang P, Beauchamp NJ. **Human brain hemorrhage: quantification of perihematoma edema by use of diffusion-weighted MR imaging.** *AJNR Am J Neuroradiol* 2002;23:1322–1326
9. Karibe H, Shimizu H, Tominaga T, Koshu K, Yoshimoto T. **Diffusion-weighted magnetic resonance imaging in the early evaluation of corticospinal tract injury to predict functional motor outcome in patients with deep intracerebral hemorrhage.** *J Neurosurg* 2000;92:58–63
10. Pierpaoli C, Barnett A, Pajevic S, et al. **Water diffusion changes in Wallerian degeneration and their dependence on white matter architecture.** *Neuroimage* 2001;13:1174–1185
11. Forbes KP, Pipe JG, Heiserman JE. **Diffusion-weighted imaging provides support for secondary neuronal damage from intraparenchymal hematoma.** *Neuroradiology* 2003;45:363–367
12. Kamal AK, Dyke JP, Katz JM, et al. **Temporal evolution of diffusion after spontaneous supratentorial intracranial hemorrhage.** *AJNR Am J Neuroradiol* 2003;24:895–901
13. Ogawa T, Okudera T, Inugami A, et al. **Degeneration of the ipsilateral substantia nigra after striatal infarction: evaluation with MR imaging.** *Radiology* 1997;204:847–851
14. Ogawa T, Yoshida Y, Okudera T, Noguchi K, Kado H, Uemura K. **Secondary thalamic degeneration after cerebral infarction in the middle cerebral artery distribution: evaluation with MR imaging.** *Radiology* 1997;204:255–262
15. Qureshi AI, Hanel RA, Kirmani JF, Yahia AM, Hopkins LN. **Cerebral blood flow changes associated with intracerebral hemorrhage.** *Neurosug Clin N Am* 2002;13:355–370
16. Nath FP, Jenkins A, Mendelow AD, Graham DI, Teasdale GM. **Early hemodynamic changes in experimental intracerebral hemorrhage.** *J Neurosurg* 1986;65:697–703
17. Bullock R, Brock-Utne J, van Dellen J, Blake G. **Intracerebral hemorrhage in a primate model: effect on regional cerebral blood flow.** *Surg Neurol* 1988;29:101–107
18. Del Bigio MR, Yan HJ, Buist R, et al. **Experimental intracerebral hemorrhage in rats. Magnetic resonance imaging and histopathologic correlates.** *Stroke* 1996;27:2312–2319
19. Power C, Henry S, Del Bigio MR, et al. **Intracerebral hemorrhage induces macrophage activation and matrix metalloproteinase.** *Ann Neurol* 2003;53:731–742
20. Nagasawa H, Kogure K. **Exo-focal postischemic neuronal death in the rat brain.** *Brain Res* 1990;524:196–202
21. Iizuka H, Sakatani K, Young W. **Neural damage in the rat thalamus after cortical infarcts.** *Stroke* 1990;21:790–794
22. Fujie W, Kirino T, Tomukai N, Iwasawa T, Tamuwa A. **Progressive shrinkage of the thalamus following middle cerebral artery occlusion in rats.** *Stroke* 1990;21:1485–1488
23. Nakane M, Tamura A, Nagaoka K, Hirakawa K. **MR detection of secondary changes remote from ischemia: preliminary observations after occlusion of the middle cerebral artery in rats.** *AJNR Am J Neuroradiol* 1997;18:945–950
24. Abe O, Nakane M, Aoki S, et al. **MR imaging of postischemic neuronal death in the substantia nigra and thalamus following middle cerebral artery occlusion in rats.** *NMR Biomed* 2003;16:152–159
25. Nakane M, Teraoka A, Asato R, Tamura A. **Degeneration of the ipsilateral substantia nigra following cerebral infarction in the striatum.** *Stroke* 1992;23:328–332
26. Forno LS. **Reaction of the substantia nigra to massive basal ganglia infarction.** *Acta Neuropathol (Berl)* 1983;62:96–102
27. Herrero MT, Barcia C, Navarro JM. **Functional anatomy of thalamus and basal ganglia.** *Child Nerv Syst* 2002;18:386–404
28. Williams PL, Warwick R. *Gray's Anatomy.* 36th ed. Edinburgh, Churchill Livingstone; 1980:1002–1044
29. Zhao F, Kuroiwa T, Miyasaka N, et al. **Characteristic changes in T(2)-value, apparent diffusion coefficient, and ultrastructure of substantia nigra evolving exofocal postischemic neuronal death in rats.** *Brain Res* 2001;895:238–244
30. Mazumdar A, Mukherjee P, Miller JH, Malde H, McKinstry RC. **Diffusion-weighted imaging of acute corticospinal injury preceding Wallerian degeneration in the maturing human brain.** *AJNR Am J Neuroradiol* 2003;24:1057–1066